PERGAMON

International Journal of Solids and Structures 37 (2000) 2285–2311

INTERNATIONAL JOURNAL OF SOLIDS and STRUCTURES

www.elsevier.com/locate/ijsolstr

Simulation of the multi-scale convergence in computational homogenization approaches

Kenjiro Terada[a,*], Muneo Hori[b], Takashi Kyoya[c], Noboru Kikuchi[d]

[a]*Graduate School of Information Sciences, Tohoku University, Aoba-yama 06, Sendai 980-8579, Japan*
[b]*Earthquake Research Institute, The University of Tokyo, Yayoi 1-1-1, Bunkyo-ku, Tokyo 113-0032, Japan*
[c]*Department of Civil Engineering, Tohoku University, Aoba-yama 06, Sendai 980-8579, Japan*
[d]*Department of Mechanical Engineering and Applied Mechanics, The University of Michigan, Ann Arbor, MI 48109-2125, USA*

Received 6 June 1998; in revised form 26 November 1998

Abstract

Although the asymptotic homogenization is known to explicitly predict the thermo-mechanical behaviors of an overall structure as well as the microstructures, the current developments in engineering fields introduce some kinds of approximation about the microstructural geometry. In order for the homogenization method for periodic media to apply for general heterogeneous ones, the problems arising from mathematical modeling are examined in the framework of representative volume element (RVE) analyses. Here, the notion of homogenization convergence allows us to eliminate the geometrical periodicity requirement when the size of RVE is sufficiently large. Then the numerical studies in this paper realize the multi-scale nature of the convergence of overall material properties as the unit cell size is increased. In addition to such dependency of the macroscopic field variables on the selected size of unit cells, the convergence nature of microscopic stress values is also studied quantitatively via the computational homogenization method. Similar discussions are made for the elastoplastic mechanical responses in both macro- and microscopic levels. In these multi-scale numerical analyses, the specific effects of the microstructural morphology are reflected by using the digital image-based (DIB) finite element (FE) modeling technique which enables the construction of accurate microstructural models.

Keywords: Homogenization methods; Periodic boundary conditions; Digital image-based modeling; RVE

1. Introduction

The mechanical behaviors of heterogeneous media essentially involve the multiple scale nature. There have been considerably many theoretical developments to obtain the reasonable estimates on the micro- (local) and macroscopic (global) mechanical behaviors within the context of mechanics of composites.

* Corresponding author. Fax: 0081 022 217 7418.
E-mail address: tei@civil.tohoku.ac.jp (K. Terada)

0020-7683/00/$ - see front matter
PII: S0020-7683(98)00341-2

Notable among the recent developments is the mathematical theory of homogenization especially for composites with periodic microstructures (see, for example, Benssousan et al., 1978; Sanchez-Palencia, 1980). The multi-scale capability of the homogenization method is recognized as a promising tool in attacking formidable problems in mechanics for heterogeneous media and, in fact, has been successfully applied to the various engineering problems for industrial composites with the help of Finite Element Method (FEM) (see, e.g., Devries and Léné, 1987; Guedes and Kikuchi, 1991; Jansson, 1993; Terada and Kikuchi, 1995; Fish et al., 1997).

The homogenization results in the mathematical theory do not impose any limitation on the microstructural composition except for the assumption of local periodicity of the media. Nonetheless, most of the results in engineering applications have involved several restrictions on the morphology of microstructures because of the lack of enough information about the microstructural geometry or the incapability of dealing with the geometrical complexity in numerical modeling. As a result, the applications in engineering problems with numerical analyses involve the idealization of microstructural heterogeneities and the simplification of the spatial distribution of inclusions. For instance, the microstructure of a fiber-reinforced composite is often assumed to have a single fiber of regular shape with surrounding matrix phase (which is sometimes called the basic structural element) and to be arranged in a periodic manner. However, in reality, many composites have more or less randomness in the geometrical configurations of constituents and even the periodic distribution of a single cell is seldom observed. Inevitable therefore, there may be potential errors in evaluating the micromechanical responses, and, as a result, in estimating the effective material properties. Such an irrelevant evaluation may not be allowable in nonlinear problems even if the periodic distribution is approximately correct and if the calculated homogenized quantities are feasible in practical applications. In fact, the errors will be accumulated and critical in estimating the overall behavior when the incremental solution method is adopted to perform fully global–local non-linear computations. Thus, the problem would be posed on the determination of a representative volume element over which the averaging is performed, on the selecting boundary conditions, and on the construction of numerical models of its heterogeneity under the assumption of local periodicity.

In this context, several attempts have been made in engineering applications. In order to include the specific effects of microstructural morphology to the homogenization analyses, Ghosh et al. (1995) utilized the Voronoi cells to represent the arbitrary distribution of inclusions and developed the novel numerical method, called the Voronoi Cell Finite Element (VCFEM). The results show good agreement with conventional and analytical solutions of plane problems in both linear elasticity and small deformation elastoplasticity. Another attempt is made by Hollister and Kikuchi (1994) to construct realistic 3-D-FE models of bone's microstructures. Their approaches extensively utilized the features of the data structure of digital images; identifying each volume picture element (voxel) as a finite element. It is shown, using the asymptotic homogenization method, that the digital image-based (DIB) modeling technique enables the quantitative study of the macro- and micromechanical characteristics of bone's porous skeleton within the framework of linear elasticity. The feasibility and applicability to the general composites have recently been studied by Terada et al. (1997), in which various usages of digital data are presented. While successfully taking into account the microstructural geometry, these studies focus their attention on the geometry modeling and tend to pay less attention to the classical notion of statistical (or macroscopic) homogeneity in defining representative volume elements (RVS's), see Hashin (1983).

Even if arbitrary morphology in the unit cell is accurately modeled by using digital images, a selected region might not necessarily be periodic in its geometry. Recently, by utilizing the convergence results in the mathematical homogenization method, Sab (1992) justified the Hill's (1963) arguments about the equivalency between displacement and traction boundary conditions on the RVE in obtaining effective material properties. Major consequence in his analysis was that 'any homogenization result that holds

for periodic media, holds also for Statistically Periodic Ergodic (SPE) and Statistically Homogeneous Ergodic (SHE) random media'. His theoretical study encourages us to examine the dependence of the macro- and micromechanical behaviors of general heterogeneous media on the selected sizes of RVEs in conjunction with the computational homogenization method for general heterogeneous media.

In this paper, we extend our current developments of the computational homogenization method for periodic media to that for general heterogeneous media whose microstructures have irregular geometrical configurations. In Section 2, we shall describe the RVE notion and the conventional homogenization with different boundary conditions, and then the variational homogenization formulae derived from the method of asymptotic expansions are briefly reviewed in the framework of linear thermo-elasticity. Assuming the periodic distribution of a single-inclusion unit cell, the numerical example shows that the periodic boundary condition gives intermediate estimates on the macroscopic quantities compared with the displacement and the traction boundary conditions. With the help of DIB FE modeling technique, Section 3 is devoted to the analysis of general heterogeneous media without assuming the geometrical periodicity for microstructures. In addition to the brief review on the mathematical theory of homogenization, it is proved that the periodic boundary condition is the best among the class of boundary conditions of RVEs. Then, the study involves the numerical simulations of the multi-scale convergence in comparison with classical approaches in RVE analyses. It is found that the homogenization method for periodic media enables the multi-scale estimates on the mechanical behaviors of general heterogeneous media without a priori assuming the geometrical periodicity. In Section 4, the nonlinear behaviors are discussed from engineering view points by examining the trends of convergence of micromechanical responses in the localization processes. The consequences in this paper would be helpful in various practical problems because the theoretical and numerical results enlarge the applicability of our current developments of the computational homogenization method.

2. The homogenization methods for periodic media

The concept of statistical homogeneity for considered media allows the introduction of a volume element over which averaging is performed meaningfully. This elementary volume is called a representative volume element (RVE) and, according to Hashin (1983), is assumed to be a cubic domain sufficiently large at the microscale and sufficiently small at the macroscale. Then the field variables such as stress and strain are also statistically homogeneous in the RVE. In the case of statistical homogeneous fields, the moving average and the ensemble average are constants and also equal, which is known as the ergodic hypothesis. In this section, based upon these classical notions for RVE, we present the analyses for overall properties of heterogeneous media. We describe the boundary value problems for RVEs so that the theoretical and technical results are briefly reviewed. After the variational formulae for computational homogenization are presented, we show some numerical simulations for actually periodic media in order to justify the theoretical results for RVE analyses in the following sections.

2.1. Classical RVE approach for effective elastic properties

In order to estimate the effective elastic properties of heterogeneous media, most of the classical methods assume the existence of a RVE. Then the RVE is subject to prescribed surface displacements (respectively tractions) which would produce a uniform strain (resp. stress) in a homogeneous medium, and eventually the linear relation between volume average stress and strain gives the overall elastic moduli. The derivation of a constitutive law involving an averaging process over RVEs is sometimes referred to as RVE analysis. Some of them are reviewed by Hashin (1983), and many micromechanics

results have been established in the framework of the RVE analyses (see, for example, Mura, 1982; Christensen, 1990; Nemat-Nasar and Hori, 1995 and references therein). Below, we briefly review the classical definition of effective elastic properties by taking after the notations by Suquet (1987, 1985) and Maugin (1992).

In the RVE analyses, two different scales are implicitly used in the description of heterogeneous media. One of these is a macroscale denoted by $\boldsymbol{x}$, at which the heterogeneities are invisible. The other is a scale for the heterogeneities and is referred to as the microscale, denoted by $\boldsymbol{y}$. The latter defines the size of the RVE whose domain is denoted by V. Then, for statistically homogeneous media, the mechanical problem is posed in the following manner: let $\boldsymbol{\sigma}(\boldsymbol{y})$ and $\boldsymbol{e}(\boldsymbol{y})$ be the stress and strain at the microscale and denote by $\langle\boldsymbol{\sigma}\rangle$ and $\langle\boldsymbol{e}\rangle$ the corresponding macroscopic quantities where the symbol $\langle\ \rangle$ indicates the volume average defined, respectively, by

$$\boldsymbol{\Sigma} := \langle\boldsymbol{\sigma}\rangle := \frac{1}{|V|}\int_V \boldsymbol{\sigma}(\boldsymbol{x},\boldsymbol{y})\,\mathrm{d}y \quad \text{and} \quad \boldsymbol{E} := \langle\boldsymbol{e}\rangle := \frac{1}{|V|}\int_V \boldsymbol{e}(\boldsymbol{x},\boldsymbol{y})\,\mathrm{d}y \tag{1}$$

where $|V|$ is the volume of the RVE. Here the strain is infinitesimal and its components are defined as

$$e_{ij}(\boldsymbol{v}) := \frac{1}{2}\left(\frac{\partial v_i}{\partial x_j} + \frac{\partial v_j}{\partial x_i}\right). \tag{2}$$

Note here that we have identified the symbol '$\boldsymbol{e}(\bullet)$' in eqn (2) with a differential operator for a vector field '$\boldsymbol{v}$' in order to distinguish the contributions from various kinds of displacement fields.

While the process that relates the $\boldsymbol{\Sigma}$ and $\boldsymbol{E}$ to the microscopic constitutive laws is called the homogenization, the inverse process that determines $\boldsymbol{\sigma}(\boldsymbol{y})$ and $\boldsymbol{e}(\boldsymbol{y})$ from $\boldsymbol{\Sigma}$ and $\boldsymbol{E}$, respectively, is called the localization. Therefore, with the data $\boldsymbol{\Sigma}$ and $\boldsymbol{E}$ in the localization process, the microscopic problem to be solved is given by

$$\begin{cases} \operatorname{div}\boldsymbol{\sigma}(\boldsymbol{y}) = \boldsymbol{0} \\ \boldsymbol{\sigma}(\boldsymbol{y}) = \boldsymbol{a}(\boldsymbol{y}) : \mathbf{e}(\boldsymbol{u}) \end{cases} \tag{3}$$

along with either one of the following boundary conditions applied to the RVE boundaries:

$$(a)\boldsymbol{\sigma}\cdot\boldsymbol{n} = \boldsymbol{\Sigma}\cdot\boldsymbol{n} \quad \text{on } \partial V$$

$$(b)\boldsymbol{u} = \boldsymbol{E}\cdot\boldsymbol{y} \quad \text{on } \partial V \tag{4}$$

where the former corresponds to the uniform traction and the latter the uniform strain. Here, '$\cdot$' makes scalar products while ':' is a trace operator.

Equivalently, in the variational formulation for (3), we can rephrase each condition by defining the solution space as a subspace of Hilbert space, $H^1(V)^3$, as follows:

$$(a')\mathscr{V}_0 = \hat{\mathscr{V}} = \left\{\boldsymbol{w}^1 \in H^1(V)^3 \,|\, \langle\boldsymbol{e}(\boldsymbol{w}^1)\rangle = \boldsymbol{0}\right\}, \tag{5}$$

$$(b')\mathscr{V}_0 = \tilde{\mathscr{V}} = \left\{\boldsymbol{w}^1 \in H^1(V)^3 \,|\, \boldsymbol{w}^1 = \boldsymbol{0} \quad \text{on } \partial V\right\}. \tag{6}$$

Here, $\boldsymbol{w}^1$ is the fluctuation of the displacement field $\boldsymbol{u}$ which has been divided as follows:

$$\boldsymbol{u} = \boldsymbol{E}\bullet\boldsymbol{y} + \boldsymbol{w}^1, \quad \boldsymbol{w}^1 \in \mathscr{V}_0. \tag{7}$$

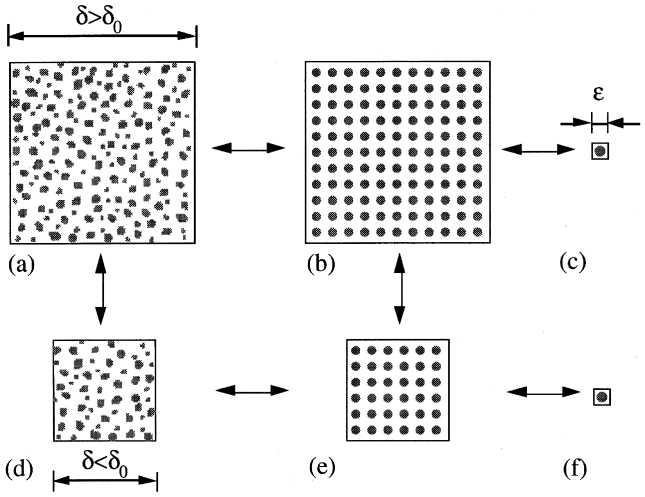

Fig. 1. Modeling of representative volume element.

When the problem is linear, the solution $\boldsymbol{w}^1$ depends linearly on the prescribed strain field, $\boldsymbol{E}$. Thus, decomposing $\boldsymbol{E}$ into six elementary states of macroscopic strains (stretch in three directions and three shears), one can write the fluctuation as $\boldsymbol{w}^1 = -\boldsymbol{\chi}^{kh}E_{kh}$, where $\boldsymbol{\chi}^{kh}(\boldsymbol{y})$ is called the characteristic deformation. Then the corresponding strain field is also given as $\boldsymbol{e}(\boldsymbol{w}^1) = -\boldsymbol{e}(\boldsymbol{\chi}^{kh})E_{kh}$ which is actually the superposition of the six elementary deformations. Thus, the strain field can be written as $\boldsymbol{e}(\boldsymbol{u}) = \boldsymbol{E} - \boldsymbol{e}(\boldsymbol{\chi}^{kh})E_{kh}$ or, in component form,

$$e_{ij} = E_{ij} - e_{ij}(\boldsymbol{\chi}^{kh})E_{kh} = s_{ij}^{kh}E_{kh}, \tag{8}$$

in which the tensor of localization has been defined as $s_{ij}^{kh} = I_{ij}^{kh} - e_{ij}(\boldsymbol{\chi}^{kh})$. Here, I_{ij}^{kh} is the fourth-order identity tensor defined as $I_{ij}^{kh} = 1/2(\delta_{ik}\delta_{jh} + \delta_{jk}\delta_{ih})$, where δ_{ij} is the Kronecker delta symbol.

By solving (3) with these two different boundary conditions, the effective elasticity compliance $\hat{\boldsymbol{A}}^H$ and stiffness tensors $\tilde{\boldsymbol{a}}^H$ can be respectively defined. In general $\hat{\boldsymbol{A}}^H$ and $\hat{\boldsymbol{a}}^H$ are not reciprocal because they are derived from different boundary conditions and the extremal principle in the calculus of variation leads to the following inequality (see, Sab, 1992 for the proof):

$$\boldsymbol{E} : \hat{\boldsymbol{A}}^H(V, \boldsymbol{a})^{-1} : \mathbf{E} \leqslant \boldsymbol{E} : \tilde{\boldsymbol{a}}^H(V, \boldsymbol{a}) : \mathbf{E} \quad \forall \boldsymbol{E} \in \boldsymbol{R}^9. \tag{9}$$

That is, the averaging process with uniform strain on the boundary overestimates the stiffness while that with uniform traction underestimates the actual one if the RVE is taken in such a manner. In this context, Hill (1967) and Mandel (1971) estimated the error between two by the relation as

$$\hat{\boldsymbol{A}}^H(\boldsymbol{V}, \boldsymbol{a}) : \tilde{\mathbf{a}}^H(V, \boldsymbol{a}) = \boldsymbol{I} + O((\varepsilon/\delta))^3 \tag{10}$$

where ε is the characteristic dimension of the heterogeneity and δ the typical size of the RVE that we have chosen. Then it was justified by Hill (1963) that 'the relationship between average strain and stress is the same for both types of boundary conditions' when δ is sufficiently large. It is expected that there may be a certain value δ_0 where effective material properties obtained from these two boundary conditions are almost reciprocal, see Fig. 1(a). Note that this holds as a consequence of statistical homogeneity of the medium.

2.2. Periodic boundary conditions

In order to introduce a priori the statistical homogeneity to the media, the local periodicity assumption of the microstructural geometry is often made (Fig. 1(b)). Then the volume element is chosen so as to contain a single inclusion in a matrix phase (Fig. 1(c)) and is therefore called a unit cell with least heterogeneity. The simplification and idealization arising from this assumption greatly reduce both numerical modeling effort and computing time because the unit cell has been chosen as a cubic cell which contains minimum morphological information.

For such a particular selection of RVE, the periodicity of the deformation might be an appropriate kinematic condition imposed on the RVE boundary. The displacement field for the microscopic problem (3) is postulated as

$$(c)\boldsymbol{u} = \boldsymbol{E}\cdot\boldsymbol{y} + \boldsymbol{w}^{\mathbf{1}},\ \boldsymbol{w}^{\mathbf{1}};\ \text{periodic},\ \boldsymbol{\sigma}\cdot\boldsymbol{n};\ \text{anti-periodic on}\ \partial V, \tag{11}$$

which is equivalent to defining the solution space such that

$$(c')\mathscr{V}_0 = \mathscr{V}_{\text{per}} = \{\boldsymbol{w}^1 \in H^1(V)^3 | \boldsymbol{w}^1;\ \text{periodic on}\ \partial V\}. \tag{12}$$

It is known that, with the help of the method of two-scale asymptotic expansions, this boundary condition makes the derivation of homogenization formulae systematic, see Benssousan et al. (1978), Sanchez-Palencia (1980).

The homogenization results obtained by this periodic boundary condition were compared by Suquet (1987) with those of the standard approaches, leading to the following relationship for the effective material properties:

$$\boldsymbol{E}:\hat{\boldsymbol{a}}^H:\mathbf{E} \leqslant \boldsymbol{E}:\boldsymbol{a}^H_{\text{per}}:\mathbf{E} \leqslant \boldsymbol{E}:\tilde{\boldsymbol{a}}^H:\mathbf{E} \quad \forall \boldsymbol{E} \tag{13}$$

where $\boldsymbol{a}^H_{\text{per}}$ is the effective stiffness matrix obtained by the periodic boundary condition and $\hat{\boldsymbol{a}}^H = (\hat{\boldsymbol{A}}^H)^{-1}$. Thus, for actual periodic media, the periodic boundary condition on the RVE of a basic structural element gives more reasonable estimation on the effective elastic moduli than both displacement and traction boundary conditions. This relationship is sometimes called the universal inequality for effective moduli for elastic media. Although this is the direct result from the inequality (9), the discrepancy between those two estimates on the effective stiffness tensors by uniform stress and strain will be significant because the characteristic length of the heterogeneity is comparable with that of unit cell, i.e., $\delta \approx \varepsilon$. Therefore, the unit cell cannot be a representative for the standard RVE analyses using these types of boundary conditions although it is a well-known fact that the periodic microstructures are statistically homogeneous.

In summary, under the assumption of periodic distribution of a basic cell with least heterogeneity, the homogenization with the periodic boundary condition can evaluate more accurate macro- and micro-mechanical behaviors in the sense that it lies in-between $\hat{\boldsymbol{a}}^H$ and $\tilde{\boldsymbol{a}}^H$. Nonetheless, owing to the estimate (10), even if the medium is periodic, the standard approaches in mechanics of materials could predict the same overall elastic properties by taking sufficiently larger RVE size (see Fig. 1). This fact was partially justified by the numerical analyses with simplified microstructures performed by Hollister and Kikuchi (1992). In this paper, this matter should be further investigated by the theoretical statements and by performing a series of computational homogenization analyses while the computations presented in this section simulate the results only for periodic media that have a single inclusion.

2.3. Variational formulation for the homogenization

Exactly the same formulae with those obtained by the microscopic problem (3) with the periodic boundary condition (12), can be derived by using the method of two-scale asymptotic expansions for piodic fields. Before carrying out the homogenization analyses, let us describe both the micro- and the macroscopic equations for linear thermo-elasticity are presented. The variational formulation for the homogenization and the localization formulae is more useful in the finite element analyses presented in this paper.

The following microscopic problems are first solved for the characteristic deformations, $\boldsymbol{\chi}^{kh}$, which contribute to the fluctuation as in (8) and that for thermal expansion, $\boldsymbol{\Psi}$, in an unit cell domain V:

$$\int_V \boldsymbol{e}_y(\boldsymbol{w}) : a : \boldsymbol{e}_y\left(\boldsymbol{\chi}^{kh}\right) \mathrm{d}y = \int_V \boldsymbol{a} : \boldsymbol{e}_y(\boldsymbol{w}) \, \mathrm{d}y \quad \forall \boldsymbol{w} \in \mathscr{V}_{\mathrm{per}}, \tag{14}$$

and

$$\int_V \boldsymbol{e}_y(\boldsymbol{w}) : \boldsymbol{a} : \mathbf{e}_y(\boldsymbol{\Psi}) \, \mathrm{d}y = \int_V \boldsymbol{\beta} : \boldsymbol{e}_y(\boldsymbol{w}) \, \mathrm{d}y \quad \forall \boldsymbol{w} \in \mathscr{V}_{\mathrm{per}} \tag{15}$$

where, $\boldsymbol{w}$ is the virtual displacement and $\boldsymbol{\beta} = \boldsymbol{a} : \boldsymbol{\alpha}$. Here $\boldsymbol{\alpha}$ is the coefficient of thermal expansion (CTE). Using these solutions, the homogenized elasticity tensor and the homogenized CTE are computed by the following formulae:

$$\boldsymbol{a}^H_{\mathrm{per}} = \frac{1}{|V|} \int_V \boldsymbol{a} : \boldsymbol{s} \, \mathrm{d}y, \quad \boldsymbol{\alpha}^H_{\mathrm{per}} = \left(\boldsymbol{a}^H_{\mathrm{per}}\right)^{-1} : \left[\frac{1}{|V|} \int_V \left(\boldsymbol{\beta} - \boldsymbol{a} : \boldsymbol{e}_y(\boldsymbol{\psi})\right) \mathrm{d}y \right] \quad \text{and} \quad \boldsymbol{b}^H = \frac{1}{|V|} \int_V \boldsymbol{b} \, \mathrm{d}y \tag{16}$$

where $|V|$ indicates the volume of the unit cell. The process up to these computations corresponds to the homogenization. Then the following macroscopic problem of the homogenized structure is solved for the averaged deformation, $\boldsymbol{u}^0(\boldsymbol{x})$:

$$\int_\Omega \boldsymbol{e}_x(\boldsymbol{v}) : \boldsymbol{a}^H_{\mathrm{per}} : \boldsymbol{e}_x(\boldsymbol{u}^0) \, \mathrm{d}x = \int_\Omega \Delta T \boldsymbol{e}_x(\boldsymbol{v}) : \boldsymbol{a}^H_{\mathrm{per}} : \boldsymbol{\alpha}^H_{\mathrm{per}} \, \mathrm{d}x + \int_\Omega \boldsymbol{b}^H \cdot \boldsymbol{v} \, \mathrm{d}x + \int_{\Gamma_t} \boldsymbol{t} \cdot \boldsymbol{v} \, \mathrm{d}\Gamma \quad \forall \boldsymbol{v} \in \mathscr{U} \tag{17}$$

where $\boldsymbol{v}$ is an arbitrary displacement defined in the admissible space

$$\mathscr{U} = \left\{ \boldsymbol{v} \in H^1(\Omega)^3 | \boldsymbol{v} = \boldsymbol{0} \quad \text{on } \partial_u \Omega = \Gamma_u \right\}. \tag{18}$$

Here $\boldsymbol{t}$ is the applied external force on the boundary Γ_t and $\boldsymbol{b}$ is the body force.

In the localization process the microscopic displacement $\boldsymbol{w}^1(\boldsymbol{x}, \boldsymbol{y})$ denotes the deformation of the unit cell and is given by

$$\boldsymbol{w}^1(\boldsymbol{x}, \boldsymbol{y}) = -\boldsymbol{\chi}^{kh} \boldsymbol{e}_{x,kh}(\boldsymbol{u}^0) + \Delta T \boldsymbol{\psi} \tag{19}$$

which corresponds to the fluctuation in Subsection 2.1. Here the subscript x indicates that the differentiation is carried out with respect to the macroscale $\boldsymbol{x}$. Therefore, once the macroscopic problem (17) is solved, the solutions, $\boldsymbol{u}^0(\boldsymbol{x})$ and $\Delta T(\boldsymbol{x})$, are localized to give the micro-mechanical responses of the unit cell. The microscopic stress field is defined by

$$\boldsymbol{\sigma}^0 = \boldsymbol{a} : \Big(\boldsymbol{e}_x(\boldsymbol{u}^0) + \boldsymbol{e}_y(\boldsymbol{w}^1)\Big) - \Delta T\big(\boldsymbol{\beta} - \boldsymbol{e}_y(\boldsymbol{\psi})\big) = \ (\boldsymbol{a} : \boldsymbol{s}) : \mathbf{e}_x(\boldsymbol{u}^0) - \Delta T\big(\boldsymbol{\beta} - \boldsymbol{e}_y(\boldsymbol{\psi})\big) \tag{20}$$

while $\boldsymbol{e}_x(\boldsymbol{u}^0) + \boldsymbol{e}_y(\boldsymbol{w}^1)$ is the microscopic strain which is identical to the expression (8).

In the above, we have skipped several steps and omitted some explanations. For the detailed derivation of the homogenization formulae, one can refer to the literature, e.g., Sanchez-Palencia (1980) and Guedes and Kikuchi (1991).

2.4. Numerical example

We shall try to justify the inequality (13) by carrying out a series of numerical experiments with three different boundary conditions on the RVE, namely the unit cell. Here we confine ourselves to actually periodic media, that is, the heterogeneous materials with a periodic microstructure. Further we assume

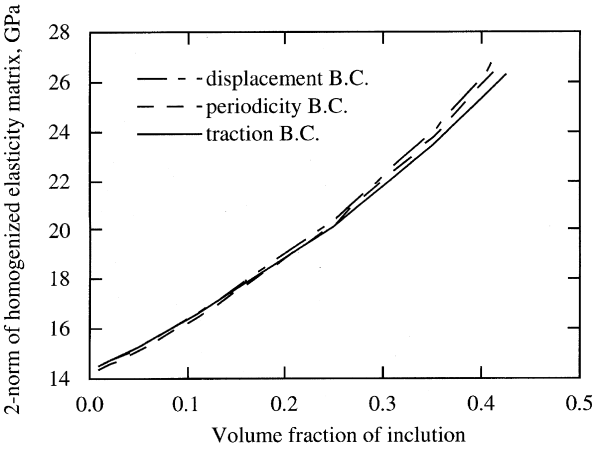

(a)

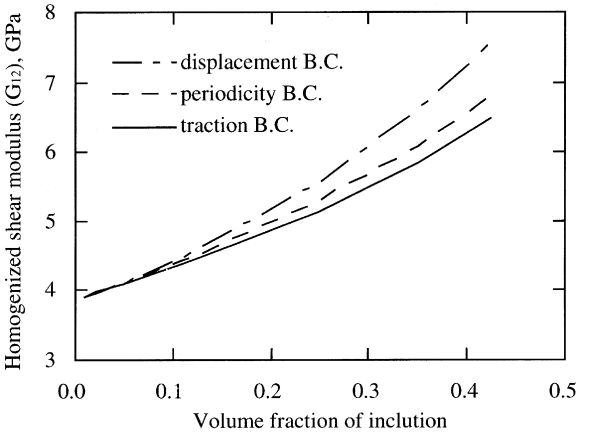

(b)

Fig. 2. Homogenized material properties vs volume fractions of inclusions: (a) in two-norm of homogenized elasticity matrix; (b) in homogenized shear modulus G_{12}.

that the heterogeneity can be idealized as a basic structural element with a single inclusion. Then the unit cell is identified with the model shown in Fig. 1(c). The material properties for each phase are given as follows: Young's modulus; 100 GPa for the inclusion, 10 GPa for the matrix; Poisson's ratio 0.3 for both.

Fig. 2 shows how the homogenized moduli change in different volume fractions of inclusion by two measures of stiffness; one is the two-norm of the homogenized elasticity matrix and the other the homogenized shear modulus. As can be seen from the figures, the actual periodic media prefer the periodic boundary condition for giving the effective material properties because the homogenization results give intermediate estimates between the ones obtained by the stress and strain boundary conditions. Of course, the term 'intermediate' is ambiguous for actual effective material properties and, in fact, there is no guarantee that it is the best among a class of possible boundary conditions. Nonetheless, the periodic boundary condition provides the reasonable estimates on the effective moduli in the sense that they are always bounded by the other. This is more rigorously confirmed from the discussions in the next section.

In spite of reasonable estimates of effective elastic properties by the periodicity assumption on the RVE geometry and the advantage in computation, many composite materials do not have such a periodic distribution of the smallest microstructural unit (Fig. 1(c)). One must suffer from the estimation errors due to the simplification and idealization of the RVE. Nonetheless, for a composite material whose microstructure has arbitrary distribution of inclusions (Fig. 1(a)), it can be proved that the asymptotic homogenization method can be applied by combining the concept of homogenization convergence and the RVE notion. This is the main subject of the following sections and the whole paper.

3. Homogenization fogeneral heterogeneous media

3.1. The mathematical homogenization theory

The mathematical theory of the homogenization method concerns composite media whose microstructure occupies a fixed region with characteristic length ε. In linear elasticity, when the medium is subjected to a certain load and given boundary conditions, the primal interest of the theory is what would happen as ε goes to zero. The theory asserts that, as ε goes to zero, the composite structure behaves as it were occupied by some equivalent homogeneous medium and that the actual displacement $\boldsymbol{u}^{\varepsilon}$ tends to the homogenized displacement field $\boldsymbol{u}^{0}$, which is a solution of the governing equations whose coefficients have been homogenized. The existence and uniqueness of the solution for the homogenization problem is owing to the notion of Γ-convergence of a functional or that of G-convergence associated with Green function (see, e.g., Zhikov et al., 1980).

In this mathematical framework, neither the microstructural configuration nor the in situ loading condition at the boundaries for microstructures are specified. Without such information, the overall elastic tensor, $\boldsymbol{a}^{\delta}$, of a cubic domain with characteristic length δ, converges to the homogenized elasticity tensor, $\boldsymbol{a}^{H}$, such that

$$\lim_{\delta \to +\infty} \boldsymbol{a}^{\delta} = \boldsymbol{a}^{H}. \tag{21}$$

However, if the concrete structure of homogenized coefficients is needed for practical uses, the homogenization method requires further information about, the kinematics, the geometry and/or the boundary conditions for the microstructure, e.g. (local) periodicity or some statistical arguments.

In this context, most of the homogenization theories have been developed particularly for periodic

microstructures (see, for example, Babuska, 1976). By assuming the periodic distribution of the basic microstructural element (unit cell), the method successfully relates micro- and macroscopic variables and, by introducing the method of two-scale asymptotic expansion, the homogenization method describes the asymptotic behaviors of composites with explicit structures of generalized convergence (see, e.g., Bensousan et al., 1978); Sanchez-Palencia, 1980; Lions, 1982; Duvaut and Nuc, 1983). This version of the homogenization, which is sometimes called the asymptotic homogenization method, allows a systematic derivation of the micro- and macroscopic problems and, therefore, is useful in numerical analyses in practical and engineering problems. Examples of such applications are found in, e.g., Devries and Léné (1987), Guedes and Kikuchi (1991), Terada et al. (1998), Kyoya et al. (1999). It is worthwhile to note that, for actual periodic media, the homogenized stiffness, $\boldsymbol{a}^H_{\mathrm{per}}$ is identical to the limit $\boldsymbol{a}^H$, in (21).

Together with the discussion in the previous section, we conclude that if the selected size of the microstructure is large enough so that the sufficient morphological information can be included, the homogenized elasticity properties are computed correctly by assuming the periodicity of field variables, but not as a geometrical restriction on the boundary. Thus, the homogenization for periodic media can be directly applied to the statistically homogeneous media by taking a large unit cell domain so that the homogenized coefficients would be so close as the H-limits, see Tartar (1989) or Sab (1992).

3.2. Periodic boundary condition for general heterogeneous media

The universal inequality (13) shows that the homogeneous stress and strain boundary conditions bound the strain energy of a body subjected to admissible boundary conditions. In this subsection, it is shown that the strain energy due to periodic boundary conditions is stationary among a certain class of strain energies.

For simplicity, consider a cube U with the edge length 2π. Let $\bar{\boldsymbol{u}}^{\boldsymbol{P}}$ and $\bar{\boldsymbol{t}}^{\boldsymbol{P}}$ be the surface displacement and traction when periodic boundary conditions are prescribed, and denote by $\boldsymbol{E}$ and $\boldsymbol{\Sigma}$ the resulting average strain and stress. Due to the uniqueness of the solution, displacement boundary conditions of $\boldsymbol{u} = \bar{\boldsymbol{u}}^{\boldsymbol{P}}$ or ∂U or traction boundary conditions of $\boldsymbol{t} = \bar{\boldsymbol{t}}^{\boldsymbol{P}}$ on ∂U are equivalent with the periodic boundary conditions. First, consider a disturbance in displacement boundary conditions, $\boldsymbol{u} = \bar{\boldsymbol{u}}^{\boldsymbol{P}} + \delta\boldsymbol{u}$ on ∂U. The change in the strain energy is $\varepsilon\bar{E}_1 + \varepsilon^2\bar{E}_2$, where $\bar{E}_1$ and $\bar{E}_2$ are functionals for $\delta\boldsymbol{u}$ and defined as

$$\bar{\boldsymbol{E}}_1(\delta\bar{\boldsymbol{u}}) = \frac{1}{U}\int_{\partial U} \bar{\boldsymbol{t}}^P \cdot \delta\bar{\boldsymbol{u}}\ \mathrm{d}S \tag{22}$$

$$\bar{\boldsymbol{E}}_2(\delta\bar{\boldsymbol{u}}) = \frac{1}{2U}\int_{\partial U} \bar{\boldsymbol{t}}(\delta\bar{\boldsymbol{u}}) \cdot \delta\bar{\boldsymbol{u}}\ \mathrm{d}S \tag{23}$$

where $\bar{t}(\delta\bar{\boldsymbol{u}})$ is surface traction when the boundary conditions are $\boldsymbol{u} = \delta\boldsymbol{u}$. Due to the periodicity of $\bar{\boldsymbol{t}}^P$, the functional $\bar{E}_1$ vanishes if the disturbance displacement is of the following form:

$$\delta\bar{\boldsymbol{u}}^P(\boldsymbol{x}) = \sum_{m_1,m_2,m_3=1}^{M} u_m \exp(\mathrm{i}\boldsymbol{m}\cdot\boldsymbol{x}) \quad (\boldsymbol{x} \text{ on } \partial U) \tag{24}$$

when u_m's are arbitrary constants and M is an arbitrary number. This $\delta\bar{\boldsymbol{u}}^P$ does not change the average strain. It follows from $\bar{E}_2 > 0$ that $\boldsymbol{u} = \bar{\boldsymbol{u}}^P$ or periodic boundary conditions yield a stationary average strain energy among the class of displacement boundary conditions.

A disturbance in traction boundary conditions can be dealt with in essentially the same manner. For

traction boundary conditions of $\boldsymbol{t} = \bar{\boldsymbol{t}}^P + \varepsilon\delta\bar{\boldsymbol{t}}$ on ∂U, the change in the strain energy is given as $\varepsilon\bar{E}_1^c + \varepsilon^2\bar{E}_2^c$ where

$$\bar{\boldsymbol{E}}_1^c(\delta\bar{\boldsymbol{u}}) = \frac{1}{U}\int_{\partial U} \delta\bar{\boldsymbol{t}} \cdot \bar{\boldsymbol{u}}\ \mathrm{d}S \tag{25}$$

$$\bar{\boldsymbol{E}}_2^c(\delta\bar{\boldsymbol{t}}) = \frac{1}{2U}\int_{\partial U} \delta\bar{\boldsymbol{t}} \cdot \bar{\boldsymbol{u}}(\delta\bar{t})\ \mathrm{d}S \tag{26}$$

with $\bar{\boldsymbol{u}}(\delta\bar{t})$ being the surface displacement when boundary conditions are $\boldsymbol{t} = \delta\bar{\boldsymbol{t}}$ (a rigid body motion is excluded). The periodicity of $\bar{\boldsymbol{u}}^P - \boldsymbol{x}\cdot\boldsymbol{\varepsilon}$ makes $\bar{E}_1^c = 0$ for a disturbance of the following form:

$$\delta\bar{\boldsymbol{t}}^P(\boldsymbol{x}) = \boldsymbol{n}(\boldsymbol{x}) \cdot \left(\sum_{m_1,m_2,m_3=1}^{M} \boldsymbol{\sigma}_m \exp(i\boldsymbol{m}\cdot\boldsymbol{x}) \right) \quad (\boldsymbol{x} \text{ on } \partial U) \tag{27}$$

with $\boldsymbol{\sigma}_0 = \boldsymbol{0}$. Since $\bar{E}_2^c$ is positive, the periodic boundary conditions yield the minimum strain energy. In other words, the periodic boundary conditions of $\boldsymbol{t} = \boldsymbol{x}\cdot\boldsymbol{\Sigma}' + \delta\bar{\boldsymbol{t}}^P$, with $\boldsymbol{\Sigma}'$ being chosen such that the average strain becomes $\boldsymbol{E}$.

It is easily seen that for any $\delta\bar{\boldsymbol{u}}^P$ (or $\delta\bar{\boldsymbol{t}}^P$), displacement boundary conditions of $\boldsymbol{u} = \boldsymbol{x}\cdot\boldsymbol{E} - \delta\bar{\boldsymbol{u}}^P$ (or traction boundary conditions of $\boldsymbol{t} = \boldsymbol{x}\cdot\boldsymbol{\Sigma} + \delta\bar{\boldsymbol{t}}^P$) yield the minimum (or maximum) strain energy, among a class of traction (or displacement) boundary conditions. However, only the periodic boundary conditions yield an average strain energy that is the minimum among the class of displacement boundary conditions and the maximum among the traction boundary conditions yield a stationary strain energy. Therefore, it can be seen that the effective elasticity tensor that is computed by using the periodic boundary conditions takes on a kind of mean value among both boundary conditions of $\{\boldsymbol{u} = \bar{\boldsymbol{u}}^P + \delta\bar{\boldsymbol{u}}^P\}$ and $\{\boldsymbol{t} = \bar{\boldsymbol{t}}^P + \delta\bar{\boldsymbol{t}}^P\}$.

The mathematical and the theoretical results described in the above are quite important in applying the computational homogenization method to practical problems. That is, in most cases, it is not easy to assure the 'sufficiently large size' of RVEs prior to the analyses. However, even if the size of unit cells depends on the capacity of our computer resources, the homogenization with periodic boundary conditions provides a reasonable approximation for the macroscopic constitutive relationship than other approaches with different boundary conditions. In other words, engineers can use the computational homogenization method with periodic boundary conditions by taking the RVE size as large as possible and need not pay much attention to the geometrical periodicity of the RVEs' boundaries.

4. The homogenization convergence in linear elasticity

4.1. Numerical modeling in conjunction with homogenization analyses

In this section, we provide the simulation of multi-scale convergence in the homogenization method based on the theoretical results presented in the previous sections. In order to perform a series of computations for this purpose, it is necessary to appropriately include the hetereogeneities of the media into the numerical analyses of homogenization. However, the computations for such convergence are not easy in general because complex geometrical modeling must be performed.

In structural analyses by the Finite Element Method (FEM), it is known that a more accurate geometry model gives better results. This is also true for microstructural analyses; the actual geometry

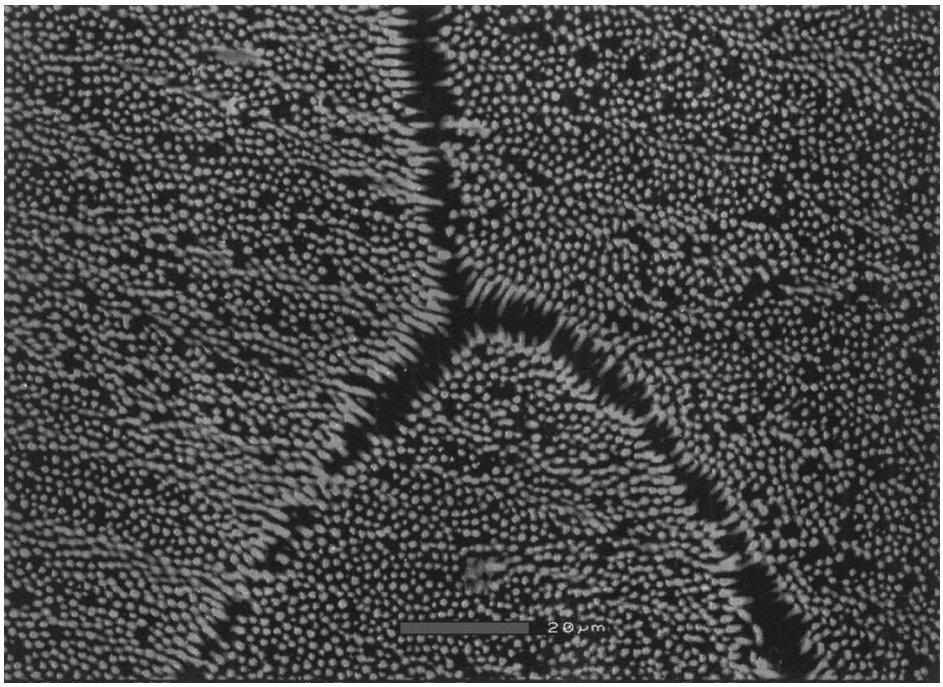

Fig. 3. Captured image (micrograph) of MMC ($NiAl_2$–Cr).

can only reproduce the actual microscopic variable fields. For instance, conventional FE geometric modeling might not give an appropriate microstructural model of naturally existing microstructures for evaluating the mechanical behaviors of an overall structure. Even for industrial composites, the idealization of the microstructural geometry seems to be irrelevant for evaluating the microscopic stress field as well as the overall mechanical behaviors. Fig. 3 shows the micrograph of a metal matrix composite whose matrix and fibers are $NiAl_2$ and Cr, respectively. It is easily imagined from the figure that the idealized geometry, e.g., the basic cell which contains a single fiber in a cubic domain, will not provide accurate stress distribution in the domain. It is, therefore, necessary to develop an accurate geometric modeling technique for the homogenization analyses.

In this paper, we are examining the applicability of the computational homogenization for periodic media to general heterogeneous media. In order to include the specific effects of microstructural morphology to the homogenization analyses, the digital image-based (DIB) modeling technique is extensively utilized because the applicability has already been justified in Hollister and Kikuchi (1994) and Terada et al. (1997). Although this numerical modeling technique plays a crucial role in this study, we provide only the procedure in the Appendix.

4.2. Simulation of the convergence of macroscopic variables

This subsection is devoted to examine the effects of the selected sizes of RVE's on the macroscopic mechanical behaviors of general heterogeneous media by carrying out a series of homogenization analyses. Keeping in mind the MMC of Fig. 3, we first made an image of a microstructure as shown in Fig. 4, which has a resolution of 1024×1024 pixels in a plane. As for the prepared microstructure, the black part is assumed to be inclusions or fibers, which have a volume fraction of $V_f = 49.0\%$, and the gray part corresponds to the matrix. Young's moduli of matrix and inclusion are $E_f = 100$ GPa and

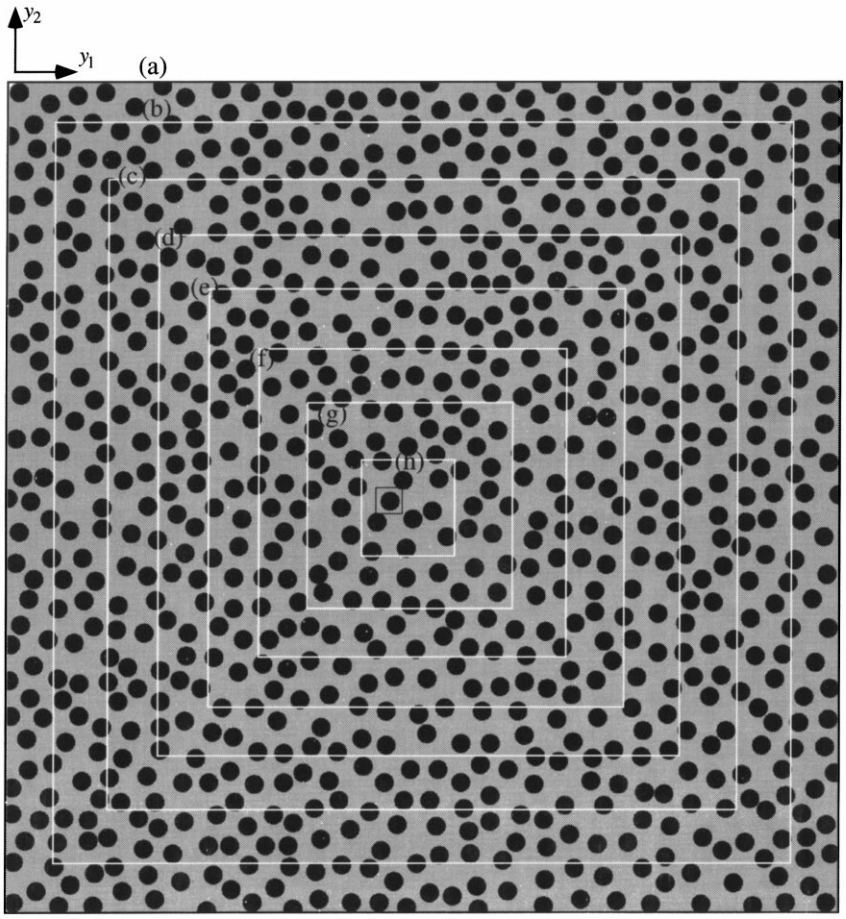

Fig. 4. Image of microstructure with selection of unit cell region: (a) 1024 × 1024; (b) 896 × 896; (c) 768 × 768; (d) 640 × 640; (e) 512 × 512; (f) 384 × 384; (g) 256 × 256; (h) 128 × 128 (pixels). (a) Digitized model (32 × 32 pixels).

$E_m = 10$ GPa, respectively, while Poisson's ratio is taken as $\nu_f = 0.3$ for both constituents. The coefficient of thermal expansion (CTE) of inclusion is given as $\alpha_f = 1.6 \times 10^{-5}/^{\circ}\mathrm{C}$ and that of matrix as $\alpha_m = 1.0 \times 10^{-6}/^{\circ}\mathrm{C}$.

The overall elastic properties, i.e., the homogenized elasticity constants and the homogenized CTE are computed by solving the microscopic problems (14) and (15) and then computing Eqs. $(16)_{1,2}$. Before studying the convergence with respect to the size of RVEs, we shall examine the feasibility of the subsequent numerical analyses. Using the material constants as specified in the above and fixing the volume fraction to $V_f = 49.0\%$, we compare the homogenized Young's modulus for the models presented in Fig. 5, which are constructed so as to be orthotropic. The digitized model has 32×32 pixels in the y_1y_2-plane so that the cell contains only a single inclusion. The results are shown in Table 1 along with those of Halpin–Tsai's analytical (semi-empirical) equations (see Halpin, 1992). Here, we have assumed that a fiber is embedded in a matrix so that the following three-dimensional effective moduli would be obtained: Young's moduli in the longitudinal and the transverse directions, E_{L} and E_{T}, respectively, and the shear modulus in the y_1y_2-plane. As can be seen from the table, the difference of

Table 1
Macro- and microscopic variables for different types of models

	E_L (GPa)	E_T (GPa)	G_{LT} (GPa)	Maximum stress (MPa)[a]	Average stress in matrix (MPa)	Average stress in inclusion (MPa)
Digitized model[b]	43.623	21.848	7.220	87.14	28.512	47.02
Idealized model	43.623	21.526	7.399	67.03	22.32	39.34
Analytical solution[c]	53.200	19.391	7.458	–	–	–

[a] Volume fraction of inclusion is 0.49.
[b] Stress values are from Case 1 (0.1% macroscopic normal strain).
[c] $E_f = E_f V_f + E_m(1 - V_f)$; $v_L = v_f V_f + v_m(1 - V_f)$; $(\bar{P}/P) = [(1 + \xi\eta V_f)/(1 - \eta V_f)]$; $\eta = [(P_f/P_m - 1)/(P_f/P_m + \xi)]$; $\bar{P} = E_T, G_{LT}, G_{LZ}$, or G_{TZ}; $\xi = 0.3$.

homogenized values computed from these two models are almost the same, say within 5%. Therefore, the error coming from discretization might be negligible in the following computations.

Next, as illustrated in Fig. 4, eight regions are selected as RVE domains, that is, the unit cells are modeled by the DIB modeling technique by changing the total number of pixels. The largest unit cell model has 1024×1024 pixels (finite elements) while the smallest model has 128×128. When changing RVE sizes in this simulation, the volume fractions must be fixed to $V_f = 49.0\%$ and the order of FE approximation should be the same for all the unit cell models. For this particular purpose, the DIB modeling technique is the most appropriate for constructing the FE unit cell model because it enables the systematic modeling for heterogeneities. In fact, the computer program developed in Terada et al. (1997) make it easy to construct the model of the same volume fraction for the RVE in Fig. 4.

The computational homogenization procedure gives the effective elasticity matrix and the homogenized CTE are, respectively, denoted by

$$\boldsymbol{a}^H = \begin{bmatrix} a^H_{1111} & a^H_{1122} & a^H_{1112} \\ & a^H_{2222} & a^H_{2212} \\ & & a^H_{1212} \end{bmatrix}, \tag{28}$$

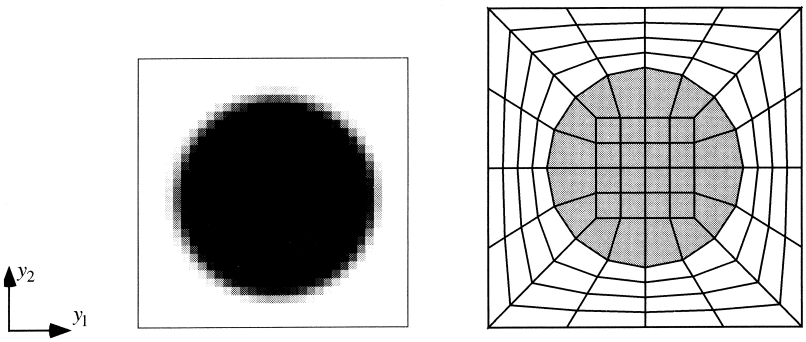

Fig. 5. DIB model and idealized finite element model.

$$\boldsymbol{\alpha}^H = \begin{bmatrix} \alpha_{11}^H & \alpha_{12}^H \\ \text{sym.} & \alpha_{22}^H \end{bmatrix}, \tag{29}$$

the former of which can be recognized as either $\hat{\boldsymbol{a}}^H$, $\tilde{\boldsymbol{a}}^H$ or $\boldsymbol{a}_{\text{per}}^H$. Fig. 6 shows the trend of convergence of two-norm of eqn (28). Here, the characteristic length in the figure indicates the length scale normalized by that of the model of 32×32 pixels (which was used in the above). It can be seen from the figure that the two-norms of homogenized elasticity matrices obtained by using periodic boundary conditions are bounded by those by the other two boundary conditions. This result agrees with those by using actually periodic microstructures in Section 2. Furthermore, all the values become close to each other as the RVE size increases irrespective of boundary conditions. In other words, there seems a limit that corresponds to the limit in eqn (21) and therefore we could simulate the converging trend of the effective elasticity properties.

Since the medium appears to be statistically homogeneous and possibly be isotropic, let us check whether or not the medium has such a feature from the computed homogenized material constants. We first define the parameters such that

$$\xi = \left| -\frac{a_{1111}^H}{a_{2222}^H} \right| \quad \text{and} \quad \Xi = \left| 1 - \frac{\alpha_{11}^H}{\alpha_{22}^H} \right| \tag{30}$$

which would be reasonable measures. For an isotropic nature of the heterogeneous media, the following measures for elasticity matrix and CTE are introduced:

$$\eta = \max\{|a_{1112}^H|, \quad |a_{2212}^H|\} \quad \text{and} \quad \Theta = |\alpha_{12}^H|. \tag{31}$$

Figs. 7 and 8 show the convergence trends associated with these parameters by taking the characteristic length normalized by the model of 128×128 pixels. As can be seen from these figures, the considered medium shows orthotropy or isotropy when the RVE sizes are taken larger and larger. It should also be noted that since the material configuration is incompatible with the periodicity at the boundary of the

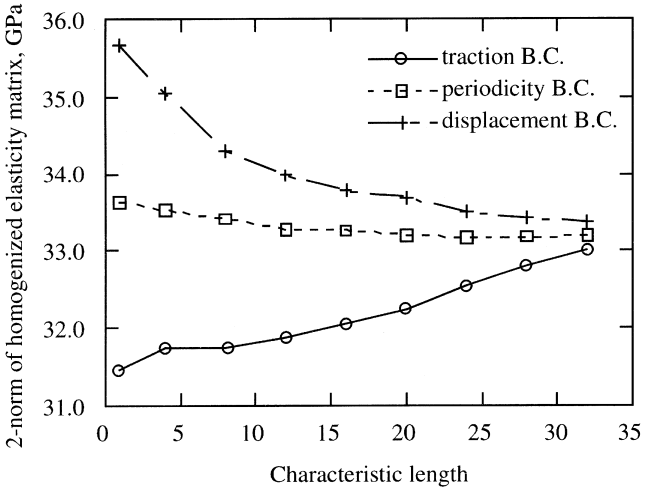

Fig. 6. Convergence associated with orthotropy and isotropy for homogenized elasticity matrix.

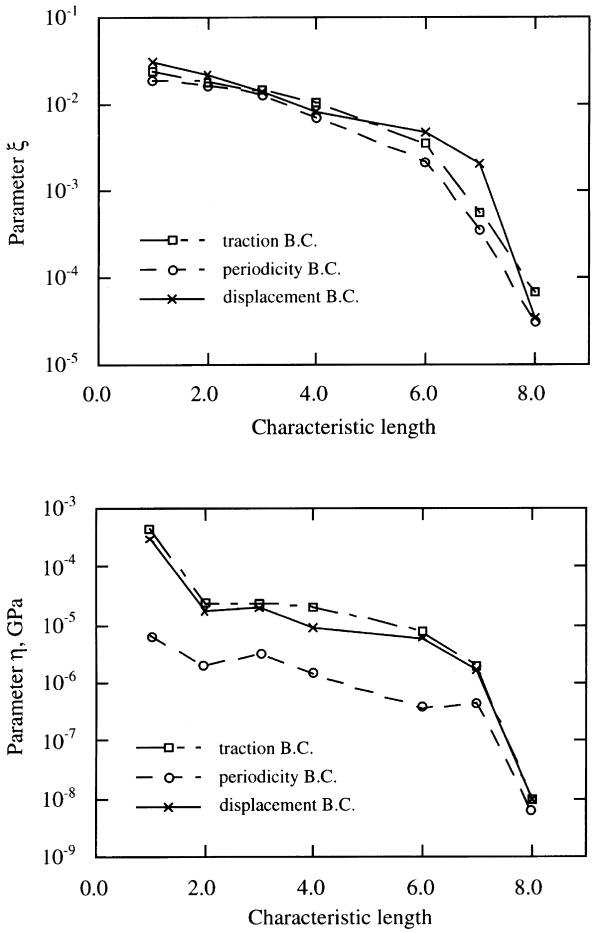

Fig. 7. Variation of two-norm of homogenized elasticity matrix with increasing RVE sizes. (a) Variation of parameter ξ for homogenized elasticity matrix. (b) Variation of parameter η for homogenized elasticity matrix.

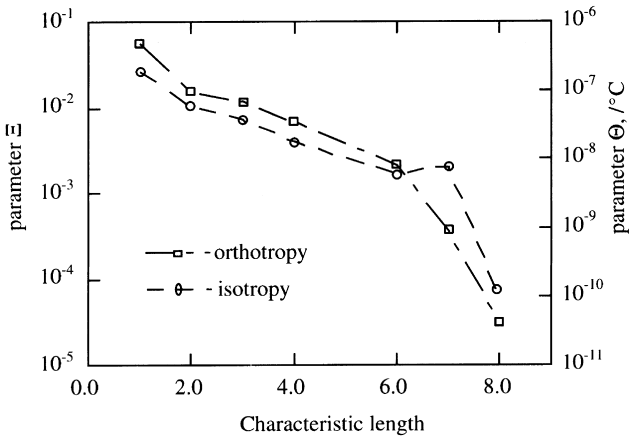

Fig. 8. Variation of microscopic stress with increasing RVE size.

RVE, there is some noises in computations. However, the influence might be limited to a thin layer near RVE's boundary and tends to disappear as the RVE size increases. This fact also proves that the statistical homogeneity along with the H-convergence could be achieved by the sufficiently large RVE as if the medium had geometrical periodicity.

In summary, the homogenization convergence of the macroscopic variables described in the above was justified by the numerical analyses. However, in this linear elasticity framework, the differences between the macroscopic values are not so large that the choice of the RVE size does not seem to cause severe error in practical applications. In other words, the periodic boundary conditions with relatively small RVE size provides reasonable estimates on the macroscopic variables for this kind of inclusion-matrix packing even if the medium does not have actual geometrical periodicity.

4.3. Simulation of the convergence of microscopic variables

On the other hand, the microscopic variables in the localization process, e.g., the microscopic stress fields eqn (20), can be evaluated for all the models. Although the localization has to be performed based on the results of macroscopic structural analyses, i.e., the solution of eqn (17), the same temperature change and strain values are applied in order to study the effects of geometric configuration and RVE sizes. In the present localization analyses, the following cases are considered:

$$\textit{Case } 1: \quad \boldsymbol{E} = \begin{bmatrix} 0.001 & 0 \\ 0 & 0 \end{bmatrix}, \quad \Delta T = 0^{\circ}\mathrm{C}$$

$$\textit{Case } 2: \quad \boldsymbol{E} = \begin{bmatrix} 0 & 0.001 \\ 0.001 & 0 \end{bmatrix}, \Delta T = 0^{\circ}\mathrm{C}$$

$$\textit{Case } 3: \quad \boldsymbol{E} = \boldsymbol{0}, \quad \Delta T = -100^{\circ}C$$

where the notations are consistent with those in Section 2. In order to make the interpretation of the micromechanical behaviors easy, von-Mises stress is mainly used as an indicator for this study. For each case, the maximum and the inclusion-averaged values of von-Mises stress is computed and these values are compared with both digitized and idealized models in Table 1. It is found from the table, the stress values computed by using the former seem to involve fairly large approximation errors. However, it is possible to compare the microscopic stresses as long as the order of approximation is kept in the DIB modeling. Thus, the computations must still be valid in the following discussions.

Fig. 9 provides the variations of the microscopic stresses as the RVE size becomes large, i.e., $\varepsilon \to 0$. Here, the characteristic length was taken with respect to the model of 32×32 pixels. As can be seen from the table and figure, the microscopic stress values also converge to certain values in the same manner as the homogenized properties of all cases. This fact, together with the convergence the macroscopic values, confirms that the nature of multi-scale convergence is observed for this heterogeneous medium.

However, the variation of the microscopic stress is much larger than that of the homogenized properties. Also, the variation of the averaged stresses in inclusions are slightly smaller than that of the maximum stresses. We recall that the homogenized properties are volume average of the microscopically distributed characteristic deformation. Although the converging variations of macro and microscopic variables are essentially equivalent, the highly oscillating stress values exist in a microscale and might be cancelled out during the averaging process for homogenization. This is probably the reason why the microscopic stress gives much larger variation in the convergence process than the macroscopic one.

The final remark is due to the study on the contour plots of microscopic stress distribution. Instead of comparing individual values of stress, let us treat them as digital images; each element value is converted

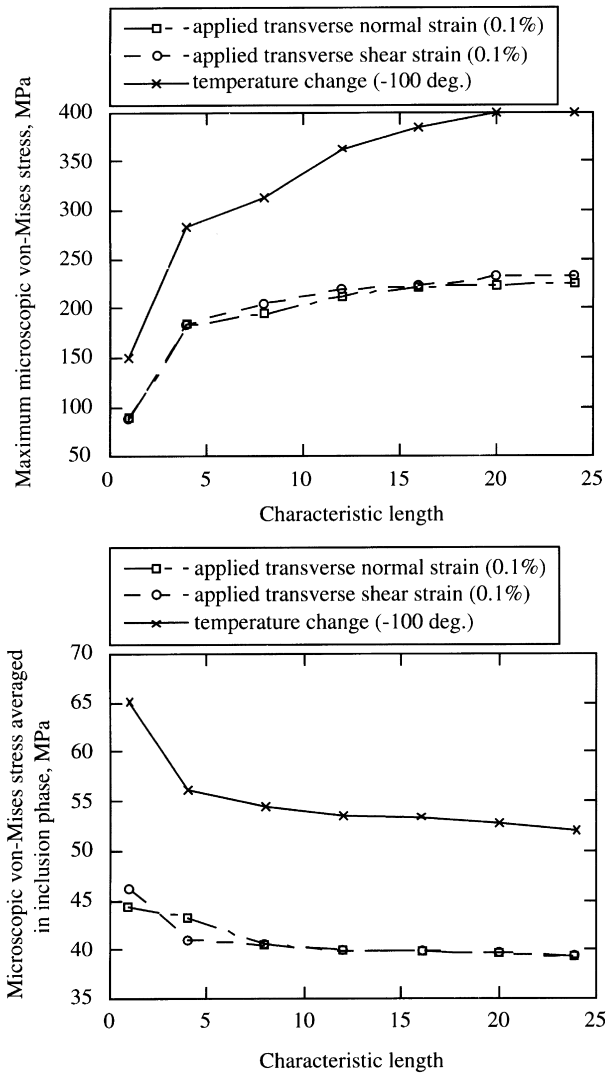

Fig. 9. Convergence associated with orthotropy and isotropy for homogenized CTE. (a) Variation of maximum microscopic stress within a unit cell. (b) Variation of difference between von-Mises stresses averaged over fibers and matrix.

to the 8-bit pixel value in the image processing software. Using this software capability, the distribution of the pixel value (0–255) in the contour enables the quantitative evaluation of the microscopic stress fields.

Fig. 10 shows stress distribution computed from the unit cell models of 32×32, 128×128 and 640×640 pixels for Case 1. Note that though the models of 128×128, 384×384 and 640×640 pixels show differences in Fig. 9, but provide similar irregularity. More specifically, the distributions (b)–(d) involve some continuous curve where the stress values are very high while (a) does not; the former three figures provide irregular distributions of microscopic stress. To this end, it is important to note that these irregular distributions of stress distinguish the idealized periodic distribution of microstructure and

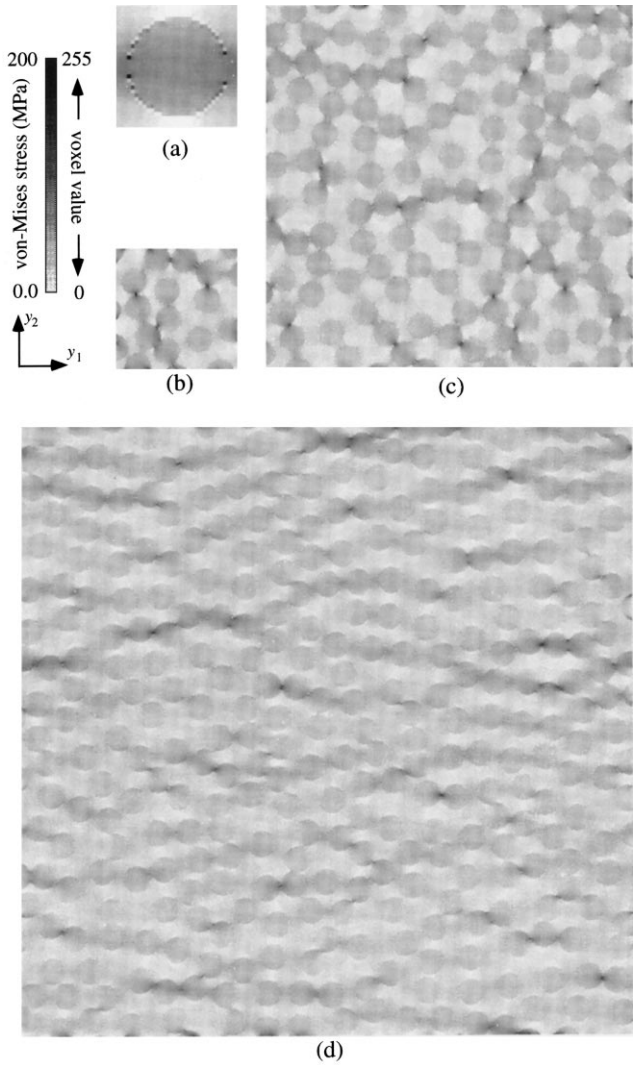

Fig. 10. Microscopic von-Mises stress distribution: (a) 32×32 (4-times enlarged); (b) 128×128; (c) 384×384; (d) 640×640 pixels.

actual microstructures. This is probably the reason why the digitized model in Fig. 5 has discrepancy in evaluating microscopic fields in Fig. 9.

The convergence results in the above are illustrative and comprehensive. However, as pointed out above, the FE approximation for the heterogeneity is not appropriate in this analysis since a single inclusion in each model does not have enough number of elements. In other words, if the microstructure that contains a single inclusion were periodically distributed like (3) of Fig. 1, the error due to the irrelevant meshing would be large. Nonetheless, the multi-scale convergent trends in Figs. 5 and 9 are still valid because the same order of approximation errors is involved in the results by the digitized models. We recall that the unit cell models were derived from the same captured image and therefore the resolution of their heterogeneities is the same order. Since the DIB modeling technique also can be a source of errors, sufficiently high resolution must be kept when the image is captured.

In conclusion, while the converging trends in both macro and microscopic variable are simulated as the size of RVE, namely unit cell, becomes large, the error due to the choice of RVE regions is much more severe in microscopic variables than in macroscopic ones. The error appears to be related to simplification and idealization of the geometric configuration of the unit cell. Since accurate evaluation of the microscopic stress is essential especially in non-linear problems, the RVE size must be taken large as much as possible when the macroscopically homogeneous nature is expected in the computational homogenization analyses.

5. Simulation of nonlinear homogenization analyses

5.1. Nonlinear mechanical behaviors of heterogeneous media

In linear elasticity framework, most of the theoretical developments for finding effective material properties do not pay much attention to the accurate evaluation of the microscopic variables. Since it is satisfactory that the overall mechanical behavior is appropriately evaluated, some kinds of approximation are introduced in the micromechanical estimation; the introduction of the phase averaged quantities or the simplification and idealization of the microstructural geometries. For instance, in the self-consistent approach by Budiansky (1965) or Hill (1965), the inclusions are embedded in a medium with the effective material properties and the Mori and Tanaka (1973) method is based on the assumption that the local fields in each inclusion can be replaced by the fields existing when the inclusion is located in a matrix phase which is subjected to the average stress or strain at infinity.

Although there must be inevitable errors in evaluating the microscopic mechanical behavior in such theoretical developments, the overall material properties do not necessarily suffer from the errors. Thus, the averaging technique not only makes the macroscopic analysis tractable but also prevents the errors in the microscopic variables from appearing in macroscopic behaviors. In fact, as studied in Section 4, the effect of RVE size on the homogenized material properties is small compared with the one for the microscopic variables.

However, the arguments for linear elasticity problems are not true for nonlinear problems. In the framework of an RVE analysis, the macroscopic mechanical responses are obtained as averaged field quantities over the RVE's and then localized to the microscopic mechanical behaviors so that the microscopic field variables are reproduced within the RVE's. Recall that, in the spirit of computational mechanics, most solution methods in numerical analyses always take the incremental (or rate) form of the variables in nonlinear problems. Therefore, the homogenization and localization processes should keep accuracy and consistency in updating each information to the next.

In this context, both mathematical and geometric modeling strategies in the microscopic problem play critical roles in nonlinear problems, such as elastoplasticity. Indeed, in the nonlinear solution method, that is, the incremental scheme in the FEM, the microscopic stress is considered as a residual (or initial) stress in the current increment. Particularly in plasticity problems, the microscopic stress at each point in the RVE domain is used to judge the yielding of the constituents. Therefore, it is necessary to accurately evaluate the whole set of microscopic (internal) variables in the RVE.

5.2. Computational homogenization analysis for elastoplasticity

The homogenization and localization for elastoplastic composite materials are discussed in terms of the notion of the self-equilibrated residual stress by Suquet (1987). According to Suquet, the residual stress is self-equilibrated i.e., $\langle \boldsymbol{\sigma}_r \rangle = \mathbf{0}$ for every RVE and, therefore, the macroscopic plastic work-rate, $\boldsymbol{\Sigma} : \dot{\mathbf{E}}^{p}$ is not necessarily equal to the average of the microscopic one, i.e.,

$$\boldsymbol{\Sigma} : \dot{\boldsymbol{E}}^{p} = \langle \boldsymbol{\sigma} : \dot{\boldsymbol{e}}^{p} \rangle + \langle \boldsymbol{\sigma}_r : \boldsymbol{a}^{-1} : \dot{\boldsymbol{\sigma}}_r \rangle. \tag{32}$$

This implies that even if we observe the macroscopic plastic strain $\boldsymbol{E}^p$, it is impossible to relate it to the microscopic one, $\boldsymbol{e}^p$, only from macroscopic approaches unless the residual elastic stress distribution within the microstructure is obtained. Thus, the direct extensions or generalizations of the linear elasticity formulations must be carefully considered.

In theoretical mechanics, the mathematical modeling of linear constitutive relations is often extended to nonlinear problems. If the approximation by such extensions is a source of errors in evaluating the microscopic variables, they are accumulated during the incremental loading. While the nonlinear versions of the self-consistent method or Mori–Tanaka method hardly reproduce the actual microscopic fields, the averaging over subcells, in the method of cells by Aboudi (1992), may fail to evaluate the accurate microscopic stress. In this sense, the constitutive modeling in the asymptotic homogenization is more reasonable since the accurate evaluation of microscopic variables is possible.

In the asymptotic homogenization method, the microscopic stress is affected by the geometrical configuration of the RVE. Therefore, the method is not free from error due to the microstructural geometry. The influence of the shapes of inclusions on the nonlinear mechanical behaviors was investigated by Guedes (1989) and Jannson (1992). They developed the computational homogenization method for two-dimensional elasplasticity and reported that the nonlinear response due to the incompressible plasticity reveals completely different trends in the macroscopic behavior after the yielding at each point in the unit cell. Such computational trends for elastoplastic composites have recently been examined in practical viewpoints by Terada and Kikuchi (1995) and Fish et al. (1997).

The morphological effects are also investigated by Ghosh and Moorthy (1995) for elastoplasticity problems by utilizing the VCFEM. However, the effects of the RVE size or the microstructural geometry on the microscopic plasticity response have not been considered. As examined in Section 4, the inappropriate RVE size for a particular material causes a more severe error in evaluating the microscopic stress in the localization process than that for macroscopic variables. In order to obtain the accuracy in the evaluation of the macroscopic deformation, it is necessary to take the large RVE size as much as possible so that the microscopic stress is accurately evaluated and the errors would be minimized.

In this section, we shall discuss the importance of the geometric modeling of the RVE in the nonlinear homogenization analysis. While the macro- and microscopic variables are successfully evaluated in the incremental solution method, the nature of the multi-scale mechanical behaviors together with the RVE geometric modeling is examined.

5.3. Convergence trend in a nonlinear problem

Based upon the formulation of the asymptotic homogenization for elastoplasticity, the numerical simulation is performed. The computational procedure follows the one found in Terada and Kikuchi (1995), but the algorithm examined in Terada et al. (1997) is also utilized for computational efficiency in the following numerical analyses.

The composite materials used here are the same MMC presented in Fig. 3, in which the fiber volume fraction is $V_f = 30\%$. We here use actual material constants of $NiAl_2$ and Cr such that Young's modulus; $E_f = 255$ GPa, Poisson's ratio; $v_f = 0.3$ for Cr fibers and $E_m = 177$ GPa, $v_m = 0.3$ for $NiAl_2$ matrix. The yield stresses are given as 150 MPa for Cr-fiber and 200 MPa for $NiAl_2$ matrix, respectively, and perfect plasticity is assumed. In order to examine the specific effect of RVE modeling, five unit cell models are used in this simulation; one is the 32×32 pixel model that has a single fiber of regular shape like Fig. 5(a) and the other four are made by selecting the following sizes of RVE's in the y_1y_2-plane: 128×128, 256×256, 512×512 and 640×640 pixels. The global structure is subjected to the uniform tensile force in the transverse direction with respect to the fiber alignment, which allows a single

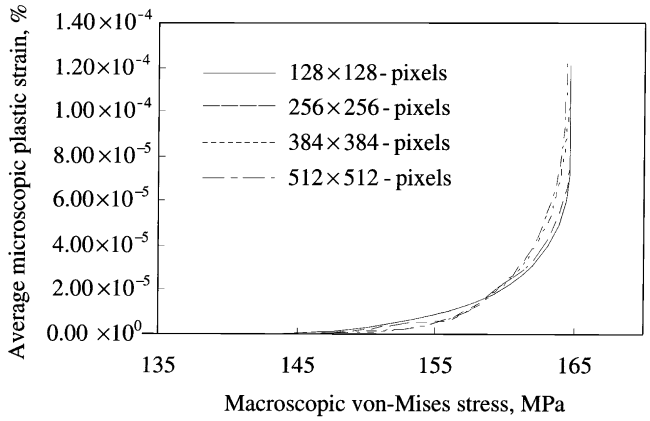

Fig. 11. Onset of plastic yielding for different unit cell sizes.

microscopic analysis in each increment. Although the analysis type presented here is simple, the qualitative discussion is possible as for the elastic–plastic behavior of heterogeneous media.

The occurrence of plastic deformation with respect to the macroscopic von-Mises stress is shown in Fig. 11. Here the equivalent plastic strain is the average within the unit cell, i.e., $\langle \boldsymbol{e}^p \rangle$, which should not be confused with the macroscopically applied deformation, $\boldsymbol{E}^p$. It can be seen from the figure, the plastic strains occur at the different macroscopic stresses. More precisely, the plastic yielding of the smaller unit cell model occurs at larger macroscopic stress value than that of larger models. This fact can be clearly observed if the macroscopic von-Mises stresses at which the plastic yielding begins are compared. In this connection, we present Fig. 12 where the characteristic length of RVE is relative to the smallest one. In the figure, as the size of the unit cell increases, the macroscopic stress at the onset of plastic yielding is reduced and appears to converge to a certain value. It is also found from Fig. 11 that the evolution of each plastic deformation also reveals a different trend from others. That is, the microscopic plastic strain of larger RVE reveals a higher accumulation rate than that of a smaller model. It is, therefore, expected that the models of larger RVE sizes tend to reveal larger macroscopic deformation for the same macroscopic external force even if the onset of plastic yielding is delayed.

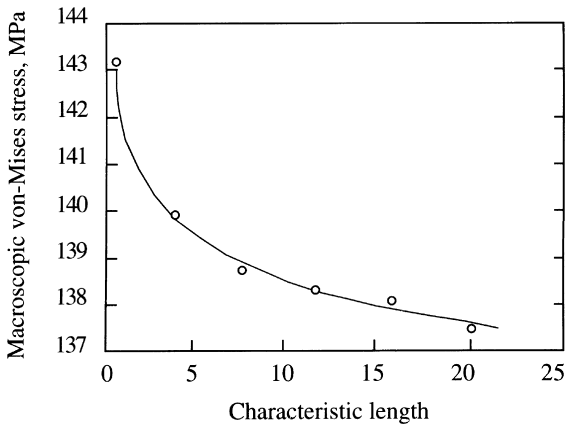

Fig. 12. RVE size vs macroscopic stress at which plastic yielding occurs.

Table 2
Average and maximum plastic strain within unit cells of different sizes at 0.2%-global elongation

Characteristic length[a]	4	8	12	16	20
Average equivalent plastic strain within unit cells ($\times 10^{-4}$)	1.290	1.322	1.341	1.352	1.359
Maximum equivalent plastic strain within unit cells ($\times 10^{-4}$)	2.501	2.870	3.669	3.830	3.911

[a] Length unit normalized by the model of 32×32 pixels.

In order to see the specific effect of the unit cell size on the microscopic deformation, let us compare the volume average and the maximum values of the microscopic strain for the digitized models by fixing the macroscopic strain by 0.2%. The results are presented in Table 2. It can be found from the table that the accumulated microscopic plastic strain within the unit cell increases as the RVE size becomes large. That is, the microscopic deformations are affected by the RVE size while the averaged deformations do not reveal much dependence. This is probably due to the fact that, according to eqn (32), the increase of the microscopic plastic strain with fixed macroscopic deformation implies the decrease of the residual stress within the unit cell. Of course, the convergence of these values can clearly be observed from Fig. 13.

As a final remark, given the size of RVE's, the multi-scale nature of the asymptotic homogenization method has enabled the accurate evaluation of both the micro- and the macroscopic variables. However, our intention is not to show the realistic analysis results but to show the importance of the geometric modeling of the RVE, especially the size effects. In fact, it is obvious from the two reasons that all of the results in this simulation are far from reality. One reason is that since the RVE size is not large enough, the asymptotic homogenization results cannot reach the H-limit. From the results for linear elasticity in Section 4, a large number of pixels in the y_1y_2-plane are required to satisfy the statistical homogeneity of the medium. Since the errors in the evaluation of the microscopic stress are very large, the homogenization method might fail to judge the yielding of constituents. Therefore, the overall deformation that is obtained by the averaging of microscopic variables cannot be the actual one. The other reason is that the FE approximation error is far from the practical tolerance since the number of finite elements that are used to form a single fiber is too small. It should be noted that the constitutive modeling of the asymptotic homogenization method provides the accurate evaluation of the nonlinear

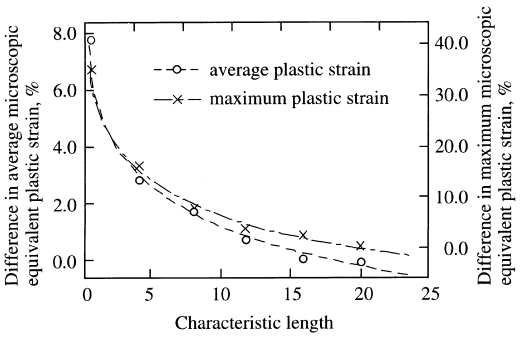

Fig. 13. Average and maximum plastic strain within unit cells of different sizes at 0.2%-global elongation (the differences indicate the deviation from the results of a 640×640-pixel model).

global-local deformations of a heterogeneous material only when the morphology of the microstructure is appropriately modeled.

In this section, the simulation of the nonlinear homogenization has been carried out in order to examine the effects of the RVE size on the micro- and the macromechanical behaviors of MMC with general heterogeneity. The dependence of microscopic deformation on both the selected region of unit cells and the microstructural morphology has been illustrated clearly with the help of the DIB modeling technique though the simulation is simple. The consequence obtained here will be significant in a fully 3-D situation because the micromechanical response at each point in the overall structure is dependent of the macroscopic deformation. In conclusion, as pointed out in Section 4, the RVE size must be taken as large as possible for accurate evaluation of nonlinear mechanical behaviors of general heterogeneous media.

6. Conclusions

In this paper, the modeling issues in the computational homogenization method were investigated in conjunction with RVE analyses of general heterogeneous media. In order for both the homogenized material properties and microscopic variables to reflect the actual microstructural geometry, the DIB modeling technique is extensively utilized to construct the numerical models of unit cells. After reviewing some theoretical results on RVE analyses, we simulated for an actual periodic medium numerically. For general heterogeneous media that reveal irregular material distribution in a microscale, it is justified theoretically that the periodic boundary condition provides the most reasonable estimates among the class of possible boundary conditions for statistical homogeneous media. Numerical simulation for those arguments also justified that the asymptotic homogenization can be applied to the analysis of general heterogeneous media by taking the unit cell size as large as possible. Moreover, it was concluded that we need not strictly require the periodicity of RVE geometry in evaluating the effective properties. This provides us with a great advantage of the computational homogenization with periodic boundary conditions over other approaches, especially in practical situations, since the results guarantee that we can utilize the computational strategies like DIB-FE modeling based on actually captured images of microstructures.

Using the asymptotic homogenization method for linear thermo-elasticity, the multi-scale convergence with respect to the RVE size was simulated and justified. Although the converging trend of the homogenized material properties is induced from the microscopic fields such as stress/strain, their convergence is slower than that of the homogenized values. It was also pointed out that the effects of the microstructural morphology especially on the microscopic stress would cause errors in evaluating the nonlinear behaviors because of the incremental schemes of the nonlinear homogenization solution method. This was demonstrated by the simulation of the elastoplastic homogenization analyses by utilizing the series of digitized meshes. Thus, it is concluded that the RVE size must be as large as possible in practical applications and that the DIB modeling is promising. Although the numerical results may be far from reality, the evolution of the computer resource capability enables the practical applications of large-scale computations involving homogenization analyses.

The FE-based asymptotic homogenization method provides reliable estimates on the micro- and macroscopic mechanical behaviors for heterogeneous media. When the nonlinear mechanical behaviors are concerned, much more attention must be paid to such a multi-scale (macro-macroscopic) nature of the mechanical responses: the mechanical behaviors for non-linear range are more sensitive to the size of RVE's than those of linear case. In conclusion, the more accurate geometric modeling of the large RVE region enables the understanding of the actual phenomena in the microscopic region as well as overall mechanical behaviors.

Acknowledgements

The authors were partially supported by NSF MSS-93-01807, US Army TACOM, DAAE07-93-C-R125 and US Navy ONR, N00014-94-1-0022 and AFOSR-URI program, DoD-G-F49620-93-0289 in the University of Michigan, and would like to thank Dr Raju Namburu and Mr Farzad Rostam-Abadi in US Army TACOM for their kind cooperation.

Appendix: Digital image-based modeling

The digital image-based (DIB) modeling technique for the FEM, which was originally developed by Hollister and Kikuchi (1994) for a study of bone microstructures, is utilized for evaluating both macro- and micromechanical response of general composite materials that is given by 2-D images, see Terada et al. (1997). The following paragraph presents the procedure of the DIB FE modeling technique for the homogenization method.

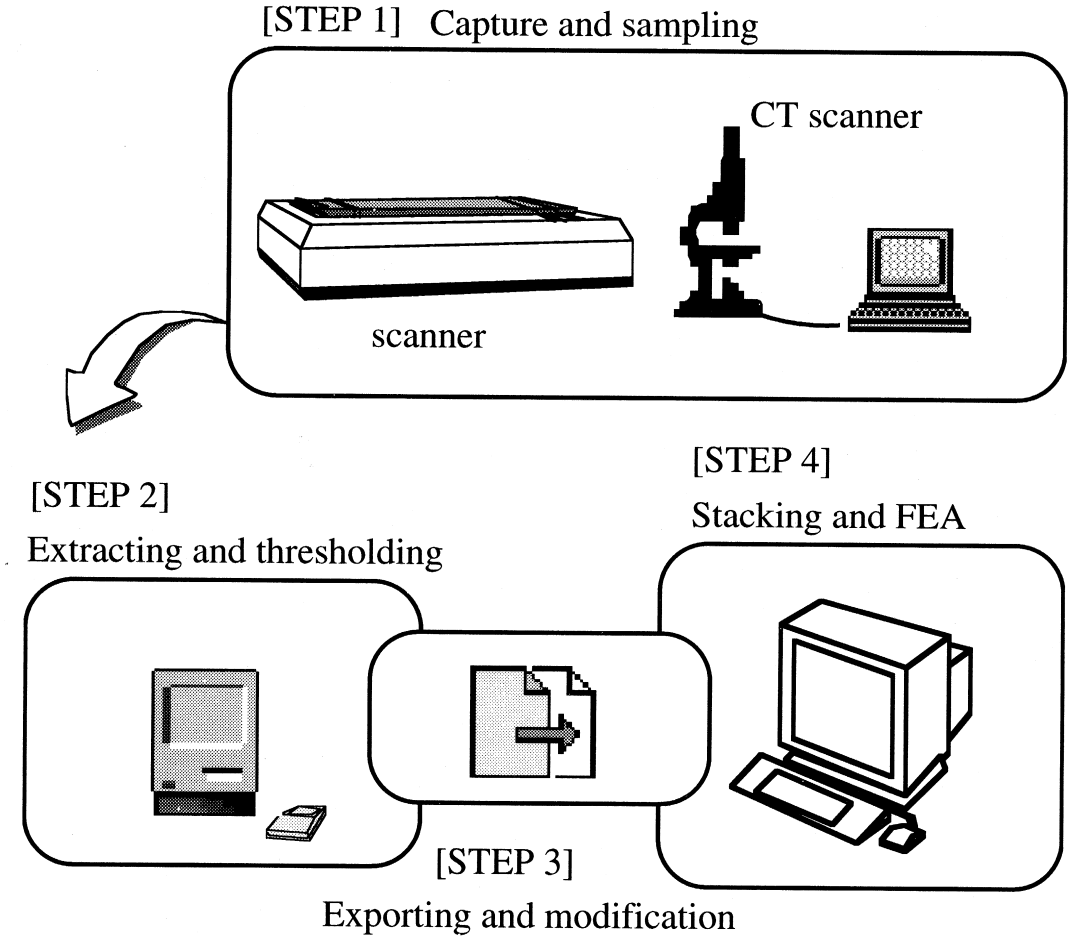

Fig. A. Procedure of DIB modeling.

The whole procedure can be divided into the following major four parts (see Fig. A):

(1) Capture and sampling: prior to digitalization, an image must be captured by an optical sensor which is chosen dependent on the desired formation modality. This process is usually assumed to be done.
(2) Selecting and thresholding: which are probably the most important operations. This process determines the unit cell size, its FE model size and the microstructural configurations. By giving the thresholding pixel value, the actual morphology such as inclusion shape, volume fractions, etc., is determined.
(3) Exporting (and adjusting, if necessary): the binary data stored in the computer are exported into an ASCII file and transferred to a UNIX platform so that our computer program can read and recognize the data. This set of data is actually the prototype of our FE model, which is either 2- or 3-D. Depending on our needs, the microstructural configuration is adjusted, e.g., the volume fraction is modified by changing the number of pixels.
(4) Stacking: prior to or during the FEA, the process is made using the exported data to construct the 3-D structure.

While the first three correspond to the pre-processing of FEA, the last process includes both the main part and post-processing of the FEA of the homogenization method. In order to construct a 3-D FE model in the DIB modeling, 2-D digital images have to be combined. The fourth process, namely the stacking, corresponds to such data operation. In 3-D FE modeling, each pixel in a 2-D image is recognized as a voxel which is identified as a finite element in FEA. For example, one can utilize a CT scanner, which can capture the inside of materials with an X-ray, and stack those into the 3-D FE unit cell model. However, microstructures of a general composite material are too small to utilize a CT scanner that has limited resolution and are usually available only on 2-D images such as micrographs. More details of the DIB modeling procedure, related image processing and applications to the homogenization analyses are found in Terada et al. (1997)

This method involves image processing which fully utilizes both hardware and software capability available. The FE model obtained in this process is the direct representation of the scanned image using, for example, two dimensionally presented micrographs of real composite materials along with image-processing software. Thus, the homogenization analyses can reflect the effects of the original geometrical configuration.

References

Aboudi, J., 1991. Mechanics of Composite Materials: A Unified Micromechanical Approach. Elsevier, Amsterdam.

Babuska, I., 1976. Homogenization and its application. Mathematical and computational problems. Numerical Solution of Partial Differential Equations. III. Academic Press, New York, pp. 89–116.

Benssousan, A., Lions, J.-L., Papanicolaou, G., 1978. Asymptotic Analysis for Periodic Structures. North Holland, Amsterdam.

Budiansky, B., 1965. On the elastic moduli of some heteronomous materials. J. Mech. Phys. Solids 13, 223–227.

Christensen, R.M., 1979. Mechanics of Composite Materials. Wiley-Interscience, New York.

Devries, F., Léné, F., 1987. Homogenization at set macroscopic stress: numerical implementation and application. Recherche Aerospatiale 1, 34–51.

Duvaut, G., Nuc, M., 1983. A new method of analysis of composite structure. Ninth European Rotor Craft Forum. Paper No. 88, Stresa, Italy.

Fish, J., Shek, K., Pandheeradi, M., Shephard, M., 1997. Computational plasticity for composite structures based on mathematical homogenization: theory and practice. Comput. Meth. Appl. Mech. Engng 148, 53–73.

Ghosh, S., Moorthy, S., 1995. Elastic–plastic analysis of arbitrary heterogeneous materials with the Voronoi cell finite element method. Comput. Meth. Appl. Mech. Engng 121, 373–409.

Ghosh, S., Lee, K., Moorthy, S., 1995. Multiple scale analysis of heterogeneous elastic structures using homogenization theory and Voronoi cell finite element method. Int. J. Solids Structures 32, 27–62.

Guedes, J.M., 1989. Nonlinear computational modeling for composite materials using homogenization. Ph.D. dissertation thesis, The University of Michigan.

Guedes, J.M., Kikuchi, N., 1991. Preprocessing and postprocessing for materials based on the homogenization method with adaptive finite element methods. Comput. Meth. Appl. Mech. Engng 83, 143–198.

Halpin, J.C., 1992. Primer on Composite Materials Analysis, 2nd. ed. Technomic.

Hashin, Z., 1983. Analysis of composite materials—A survey. J. Appl. Mech 50, 481–505.

Hill, R., 1963. Elastic properties of reinforced solids: some theoretical principles. J. Mech. Phys. Solids 11, 357–372.

Hill, R., 1965. A self consistent mechanics of composite materials. J. Mech. Phys. Solids 13, 213–333.

Hill, R., 1967. Essential structure of constitutive laws for metal composites and polycrystals. J. Mech. Phys. Solids 15, 79–95.

Hollister, S.J., Kikuchi, N., 1992. A comparison of homogenization and standard mechanics analysis for periodic microstructure. Comput. Mech. 10, 73–95.

Hollister, S.J., Kikuchi, N., 1994. Homogenization theory and digital imaging: a basis for studying the mechanics and design principles of bone tissue. Biotech. Bioengin. 43 (7), 586–596.

Jansson, S., 1992. Homogenized nonlinear constitutive properties and local stress concentrations for composites with periodic internal structure. Int. J. Solids Structures 29, 2181–2200.

Kyoya, T., Terada, K., Kawamoto, T., 1999. Multi-scale limit load analysis of discontinuous rock mass based on the homogenization method. Int. J. Numer. Anal. Meth. Geomech. 23, 995–1019.

Lions, J.-L., 1982. On some homogenization problems. Zeitschrift fur Angewandte Mathematik und Mechanik 62, 251–262.

Maugin, G.A., 1992. The Thermomechanics of Plasticity and Fracture. Cambridge University Press.

Mori, T., Tanaka, K., 1973. Average stress in matrix and average energy of materials with misfitting inclusions. Acta Metall. Mater. 21, 571–574.

Mura, T., 1982. Micromechanics of Defects in Solids. Martinus Nijhoff.

Nemat-Nasser, S., Hori, M., 1993. Micromechanics: Overall Properties of Heterogeneous Materials. North-Holland, Amsterdam.

Sab, K., 1991. Principe de Hill et homogénéisation des matériaux aléatoires. C. R. Acad. Sci. Paris Serie II 312, 1–5.

Sab, K., 1992. On the homogenization and the simulation of random materials. Eur. J. Mech. A/Solids II 5, 585–607.

Sanchez-Palencia, E., 1980. Non-homogeneous Media and Vibration Theory. Lecture Notes in Physics 127. Springer-Verlag, Berlin.

Suquet, P.-M., 1985. Local and global aspects in the mathematical theory of plasticity. In: Sawczuk, A., et al. (Eds.), Plasticity Today. Elsevier, London, New York, pp. 279–309.

Suquet, P.-M., 1987. Elements of homogenization theory for inelastic solid mechanics. In: Sanchez-Palencia, E., Zaoui, A. (Eds.), Homogenization Technique for Composite Media. Springer-Verlag, Berlin, Heidelberg, New York, pp. 194–275.

Tartar, L., 1989. H-measures and small amplitude homogenization. In: Kohn, R., Milton, G. (Eds.), Random Media and Composites. SIAM Proceeding Series, pp. 89–99.

Terada, K., Kikuchi, N., 1995. Nonlinear homogenization method for practical applications. In: Ghosh, S., Ostoja-Starzewski, M. (Eds.), Computational Methods in Micromechanics, AMSE, AMD, vol. 212, pp. 1–16.

Terada, K., Ito, T., Kikuchi, N., 1998. Characterization of the mechanical behaviors of solid–fluid mixture by the homogenization method. Comput. Meth. Appl. Mech. Engng 153, 223–257.

Terada, K., Miura, T., Kikuchi, N., 1997. Digital image-based modeling applied to the homogenization analysis of composite materials. Comput. Mech 20, 331–346.

Terada, K., Suzuki, K., Ohtsubo, H., 1997. FFT-based homonization algorithm using digital images. Mater. Sci. Res. Internat. 3, 231–236.

Zhikov, V.V., Kozlov, S.M., Oleinik, O.A., 1995. Homogenization and Differential Operators and Integral Functionals. Springer-Verlag, New York.